phys. stat. sol. (b) **140**, 311 (1987)

Subject classification: 78.55; 78.65; S6

Fachbereich Physik der Universität Marburg[1]

Photoluminescence in a-$Si_{1-x}C_x$:H Films

By

W. SIEBERT, R. CARIUS, W. FUHS, and K. JAHN

A study of steady-state and time-resolved photoluminescence (PL) and optical properties of a-$Si_{1-x}C_x$:H-films prepared by glow-discharge decomposition of gas mixtures of SiH_4 and CH_4 is presented. With increasing carbon content x the PL-spectra shift to higher energies and broaden considerably. Simultaneously the quantum efficiency decreases at low x but increases again above $x \approx 0.6$. The PL-decay after pulse excitation (10 ns) is enhanced with increasing x, the lifetime spectra shift to shorter times by more than two orders of magnitude ($x < 0.45$). The data indicate a strong decrease of the average radiative lifetime with x. This behavior is explained by an enhancement of the Coulomb attraction between the recombining carriers and/or faster thermalization in the band tails.

Die Arbeit berichtet über eine Untersuchung von optischen Eigenschaften, der stationären und zeitabhängigen Photolumineszenz von amorphen Filmen aus a-$Si_{1-x}C_x$:H, die durch Plasmadeposition aus Gasgemischen von Silan und Methan hergestellt werden. Mit zunehmendem Gehalt an Kohlenstoff verschieben sich die Spektren zu höherer Energie und verbreitern erheblich. Die Quantenausbeute fällt dabei mit steigendem x ab. Das Abklingen der PL nach Pulsanregung wird durch Einbau von Kohlenstoff stark beschleunigt, die Lebensdauerspektren verschieben sich um mehr als zwei Größenordnungen zu kürzeren Zeiten ($x < 0{,}45$). Die Ergebnisse deuten auf eine starke Abnahme der mittleren Lebensdauern für strahlende Rekombination hin. Dieses Verhalten wird durch die Verstärkung der Coulombwechselwirkung zwischen den Rekombinationspartnern und/oder schnellere Thermalisierung in den Tailzuständen erklärt.

1. Introduction

Since the first report on the electronic properties of glow discharge deposited amorphous silicon-carbide alloys [1] this material has attracted a great deal of interest owing to possible applications in optoelectronic devices [2 to 4]. Alloying of silicon with carbon is known to widen the energy gap. Unfortunately this is accompanied by a degradation of electronic properties such as photoconductivity, photoluminescence efficiency, which is due to the creation of additional defects [5, 6]. This tendency for defect creation might arise from differences in bond length, the tendency of C atoms for threefold coordination, or the incorporation of hydrogen in the film. The latter is expected even to change the microstructure of the films by inducing an open void structure [7].

In order to obtain information on the recombination processes in a-SiC:H we have studied the steady-state and time-resolved photoluminescence in these alloys. Our samples were prepared by the glow discharge method using undiluted gas mixtures of silane and methane and have already been characterized chemically and structurally elsewhere [7].

The cw spectra of a-SiC:H [8], a-SiN:H [9, 10], and a-SiO:H [11] have been reported to shift to higher energy and to broaden with increasing content of alloying atoms.

---

[1] Renthof 5, D-3550 Marburg, FRG.

They consist of one band in the entire composition range. These results suggest that the main recombination mechanism is not drastically altered by alloying [8, 9] and that the observed changes are predominantly due to (i) an increase of the optical band gap, (ii) a broadening of the band tails, and (iii) an increase of the defect density with alloying. Most of the results therefore have been discussed in terms of models that have been developed for recombination in a-Si:H [13]. Preliminary data on time-resolved measurements [12] indicated a pronounced decrease of the radiative lifetime with the carbon content x in a-$Si_{1-x}C_x$:H alloys. In this paper we present additional data which support this conclusion.

2. Film Preparation and Characterization

The samples were prepared by glow discharge decomposition of undiluted mixtures of silane (SiH_4) and methane (CH_4) in a capacitively coupled system using the following parameters: substrate temperature 250 °C, pressure 0.1 to 0.2×10^2 Pa, gas flow 2 to 25 sccm, rf power 10 W. The deposition rate was found to decrease from 0.32 mm/s in a-Si:H to about 0.05 mm/s in a-$Si_{1-x}C_x$:H with $x = 0.87$. The film thicknesses ranged from 0.5 to 1.15 μm. In order to avoid interference effects the films for luminescence measurements were deposited on roughened substrates.

A detailed report of the structural and compositional characterization of these films has recently been published [7]. This study included Auger electron spectroscopy (AES), hydrogen effusion, and infrared absorption. It is found that the carbon content in the film x rises only slowly with the gas phase ratio methane/silane up to ratios of about 0.8 but increases much more strongly at higher values. An important result is that the hydrogen content, C_H, increases appreciably with increasing x, from 12 at% in a-Si:H to about 50 at% at $x = 0.4$. Connected with this tremendous enhancement of C_H is a change in the microstructure of the films. Hydrogen effusion studies strongly suggest that a-$Si_{1-x}C_x$:H films, in particular those with $x > 0.2$, contain a void structure. This manifests itself also in a drastic decrease of the photoconductivity. These observations are consistent with the quite generally reported strong increase of the defect density with x (see e.g. [5]). The studies of effusion and IR absorption have also suggested that it is solely the carbon content that determines the hydrogen content in the films. This is supposed to be due to the larger binding energy of C–H (3.5 eV) compared to that of Si–H (3.1 eV).

3. Experimental Results

Fig. 1 displays absorption spectra which were derived from measurements of transmission and reflectivity. With increasing x the absorption curves shift to higher energy indicating the increase of the optical band gap. As a measure for the band gap we take E_{04}, the energy at which the absorption coefficient amounts to 10^4 cm^{-1}. An almost linear increase of E_{04} up to the highest values of x is observed. At low carbon content x the shift occurs with only minor changes of the slope. At higher x, however, the curves clearly flatten, which points to an increasing width of the band tails. These changes in the absorption spectra cause a steady decrease of the refractive index and dielectric constant with x (Fig. 2). The quantities plotted in Fig. 2 were evaluated from transmission interference fringes at photon energies where the absorption coefficient was less than 10^3 cm^{-1}. Similar behavior has been reported by others [8].

The measurements of the cw luminescence were performed at 77 K using a tunable dye laser system in the energy range 1.55 to 2.2 eV and the lines of a krypton laser

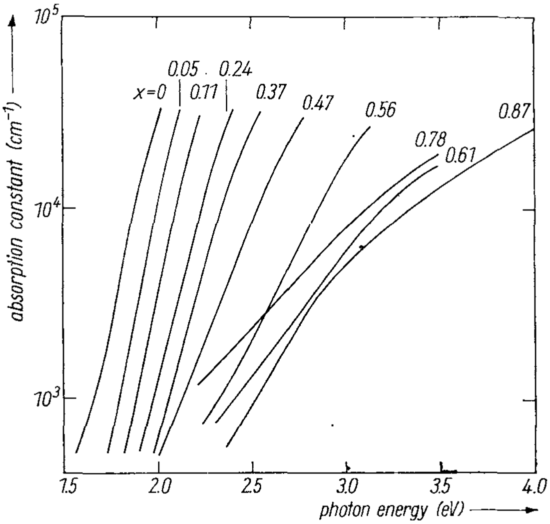

Fig. 1. Absorption edges of a-$Si_{1-x}C_x$:H films at various compositions x

for excitation at higher energies. In order to account for the different values of the band gap, the excitation energy E_{ex} was chosen equal to E_{04}. The excitation density was kept less than 2×10^{18} cm^{-3} s^{-1}. Under such conditions the recombination kinetics are excpected to be monomolecular [14]. The luminescence light was analysed by a double prism monochromator and all spectra were corrected for the spectral response of the whole detection system.

Fig. 3 shows normalized cw emission spectra in the composition range $0 \leqq x \leqq \leqq 0.82$. The spectra exhibit a one-band structure and are approximately symmetrical. With increasing x the spectra shift to higher energy and broaden considerably. The luminescence peak energy E_{PL} increases almost linearly with x but this increase is less pronounced than that of the band gap E_{04} suggesting a widening of the band tails. In Fig. 4 three quantities are plotted as a function of composition x which are related to the width of the band tails: $\frac{1}{2}$ (E_{04} — E_{PL}), the full width at half maximum E_{FWHM} of the emission bands in Fig. 3, and the reciprocal logarithmic slope $\Delta E/\Delta \lg \alpha$ of the absorption curves at $\alpha \approx 10^4$ cm^{-1} (Fig. 1). Although the detailed relation of these quantities to the band tail width is rather complicated, their continuous increase with x strongly points to a broadening of the band tails by alloying. It is important to note, however, that at low x this effect is much less pronounced than at higher carbon

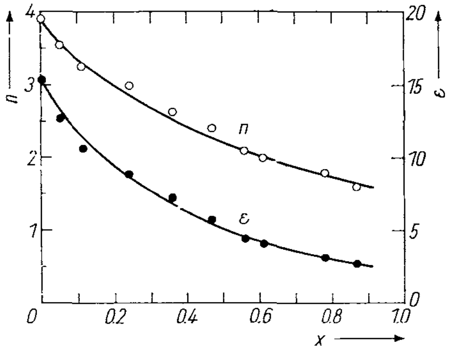

Fig. 2. Refractive index n and dielectric constant ε as a function of composition x

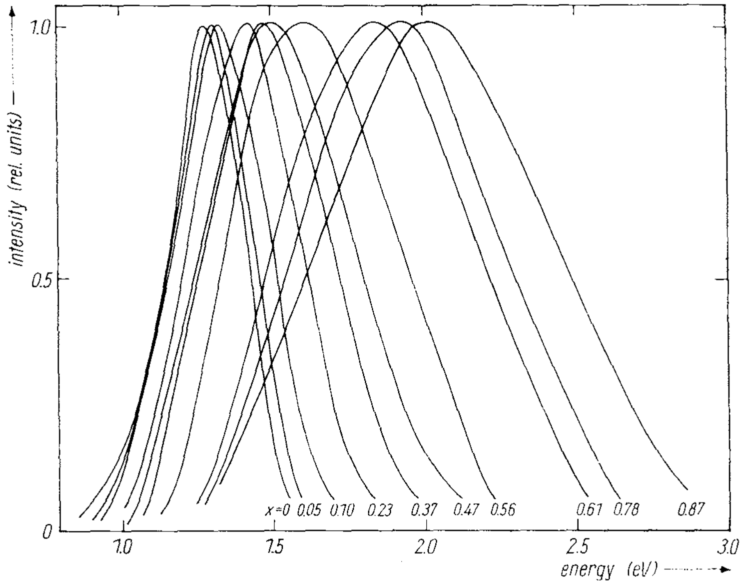

Fig. 3. Normalized photoluminescence spectra of a-$Si_{1-x}C_x$: H for various values of x at $T = 77$ K

contents ($x > 0.2$). Different from our results, Sussman and Ogden [8] found a maximum of E_{FWHM} at $x \approx 0.7$. This may arise from the fact that the excitation energy in this study did not exceed 2.8 eV which is considerably less than E_{04} in films of $x = 0.7$. It will be shown below that excitation with $E_{ex} < E_{04}$ results in a decrease of both E_{PL} and E_{FWHM}.

In a-Si:H the photoluminescence spectra do not depend on the excitation if E_{ex} is larger than the band gap derived from a Tauc plot. For lower E_{ex} the spectra shift to lower energy without noticeable change in halfwidth [15]. This is different from the behavior of the alloys. Fig. 5 shows as an example the influence of sub-band gap excitation on the spectra of a film with $x = 0.5$. For $E_{ex} < 2.2$ eV there is clearly a red shift of the spectrum but also a decrease of the halfwidth from 0.48 eV at $E_{ex} > 2.2$ eV to 0.4 eV at $E_{ex} = 1.85$ eV. For the pure a-C:H film, this effect is much more pronounced. The halfwidth decreases from 0.9 eV for $E_{ex} = 3.5$ to 0.4 eV at $E_{ex} = 1.97$ eV. Additionally the spectra become asymmetric, i.e. steeper, at the high-energy side whereas the low-energy side remains unchanged. Fig. 6 shows that

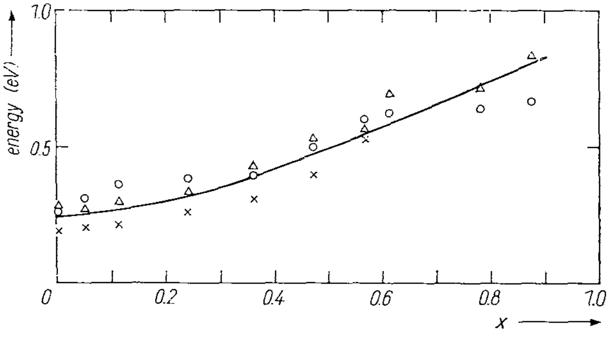

Fig. 4. Quantities which are related to the width of the band tails as a function of composition x (details see text). ○ $\frac{1}{2}(E_{04} - E_{PL})$, △ E_{FWHM}, × $\Delta E/\Delta \lg \alpha$

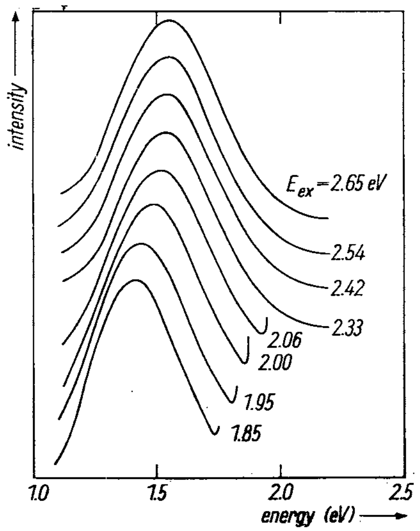

Fig. 5. Photoluminescence spectra of a-$Si_{0.5}C_{0.5}$:H at various values of the excitation energies E_{ex}. $E_{04} = 2.54$ eV

the shift of the peak energy is roughly proportional to the change of E_{ex}. Although a slope is hard to define the trend of an increasing slope is obvious. A similar behavior has been reported for a-SiN_x:H films recently [16] with slopes ranging from 0.5 to 1 and has been discussed in terms of a thermalization model.

The quantum efficiency η was determined by comparing the integrated emission intensity with that of a high quality a-Si:H sample. The quantum efficiency η_{Si} of this reference amounted to about 30% at 50 K. In accordance with other authors [17, 18] we find that the quantum efficiency decreases strongly with alloying at low x indicating the enhancement of the density of defect states (Fig. 7). Near $x \approx 0.5$ a minimum value is indicated. An increase on the carbon-rich side of the alloy system has been reported by Sussman and Lauder [19]. It is important to note that the efficiency determined from pulse experiments agrees fairly well with the values obtained from steady-state measurements. To obtain a measure for the number of emitted photons per pulse, N, the decay curves (Fig. 8a) have been integrated from 10^{-8} s to the time after which the intensity has dropped to 10^{-6} of the initial value I_0 ($t = 10^{-8}$ s). Then the quantum efficiency is defined by the ratio $\eta = N/N_0$, where

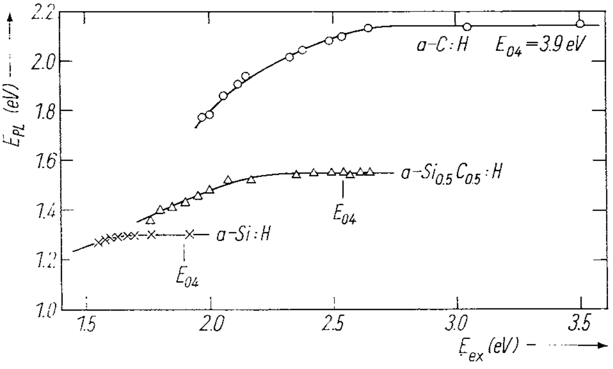

Fig. 6. Peak energy E_{PL} of the photoluminescence spectra as a function of excitation energy E_{ex} at $T = 77$ K

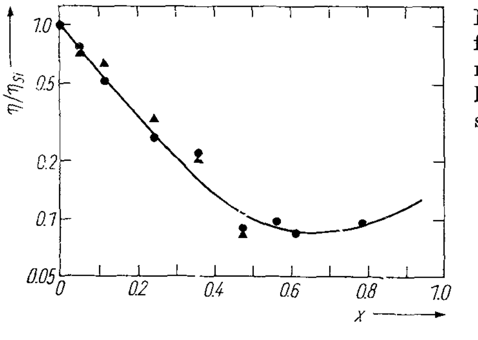

Fig. 7. Quantum efficiency of a-$Si_{1-x}C_x$:H as a function of x at $T = 77$ K. ● from cw measurements, ▲ from time-resolved data. η is plotted relative to the efficiency of a high quality a-Si:H sample

N_0 is the number of generated electron–hole pairs per pulse. We also studied the temperature dependence of the efficiency and found the same behavior as reported in the literature [19]. With increasing x the temperature dependence becomes progressively less pronounced and even vanishes for films of high carbon content.

More detailed information about the radiative and non-radiative recombination processes can be obtained from time-resolved studies. We have investigated therefore the decay of the photoluminescence intensity following a short (10 ns) excitation pulse.

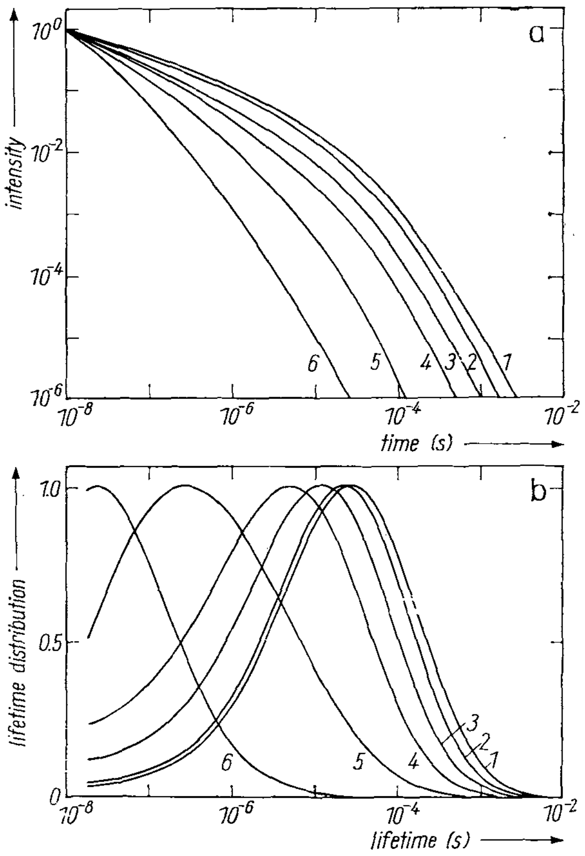

Fig. 8. a) Luminescence decay and b) lifetime distribution of a-$Si_{1-x}C_x$:H at $T = 77$ K for various compositions x. (1) $x = 0$, (2) 0.05, (3) 0.1, (4) 0.23, (5) 0.37, (6) 0.47

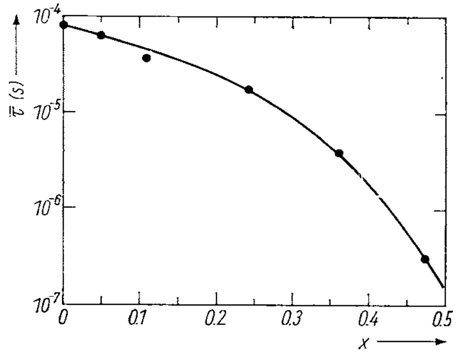

Fig. 9. Average lifetime $\bar{\tau}$ as a function of composition x (calculated from the data in Fig. 8b) at $T = 77$ K

The decay was recorded by a boxcar integrator and constructed from six sets of data on different time scales. Since the response time of the detection system was about 15 ns the study was limited to films of carbon content below $x = 0.47$. Fig. 8a shows normalized decay curves (total photoluminescence) at various compositions x. With increasing x the decay is enhanced but the general form of the curve remains similar to that of a-Si:H which shows that there is no drastic change in the recombination mechanism by alloying. In Fig. 8b the lifetime distributions are plotted which have been calculated from the decay curves following the procedure described by Tsang and Street [20]. The result is a broad spectrum of lifetimes extending over about five orders of magnitude which is typical of tunneling recombination. With increasing carbon content x the lifetime distribution shifts strongly to shorter times. This is in principle what one would expect from an enhancement of the non-radiative channel. It will be shown below, however, that the shift arises predominantly from a decrease of the radiative lifetime with x. Fig. 9 shows that the average radiative lifetime $\bar{\tau}$, which roughly corresponds to the peak position of the distribution curves, decreases from 8×10^{-5} s in a-Si:H to 3×10^{-7} s at $x = 0.47$.

Measurements of the luminescence spectra at fixed delay times after excitation yield information about the energy distribution of the recombining carriers as well as about thermalization and relaxation processes. The time-resolved spectra show a substantial and non-monotonic shift of the peak energy with delay time but the

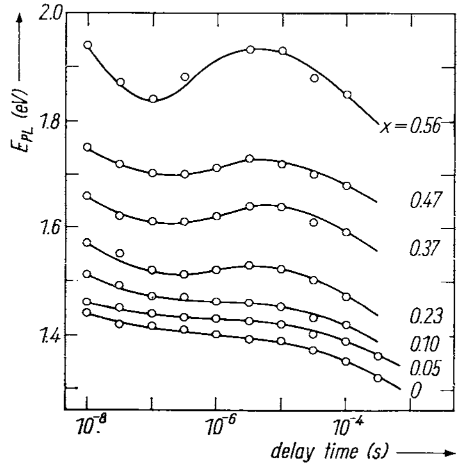

Fig. 10. Time-resolved shift of the luminescence peak energy E_{PL} at various compositions x ($T = 77$ K)

shape and halfwidth remain essentially unaffected. In the dependence of E_{PL} on the delay time clearly three time ranges can be identified (Fig. 10). In the short time region ($t < 10^{-7}$ s) thermalization of the excited carriers in the band tails prevails and E_{PL} decreases with time as the carriers lose energy. This process becomes more pronounced for higher x. In the medium time range (10^{-7} s $< t < 5 \times 10^{-6}$ s) E_{PL} remains almost constant at low x but increases with time for $x > 0.1$. Such a behavior has been interpreted by Coulomb attraction between the recombining carriers [20]. In terms of this model the results in Fig. 10 indicate stronger Coulomb attraction in carbonated films which is consistent with the decrease of the dielectric constant shown in Fig. 2. Finally, for delay times above about 5×10^{-6} s, E_{PL} decreases for all values of x. This decrease is more pronounced at higher carbon contents. Similar variations of E_{PL} have been found in other silicon alloys such as a-SiN$_x$:H [9] or a-SiO$_x$:H [9, 21].

4. Discussion

The similar behavior of a-Si:H and the a-Si$_{1-x}$C$_x$:H alloys shows that alloying does not alter drastically the dominant recombination mechanism. We therefore discuss the results in terms of the models developed for a-Si:H [13]. After excitation the carriers thermalize in their respective band tails from which they either recombine by radiative tunneling with the carriers in the other band tail or by non-radiative tunneling via defect states. In a-Si:H the Si dangling bonds are believed to be the most important centers for non-radiative recombination [13]. The radiative lifetime depends exponentially on the separation between the recombining carriers,

$$\tau_r = \tau_0 \exp\left(\frac{2R}{R_0}\right). \tag{1}$$

In this expression R_0 is the Bohr radius of the more extended wave function which is considered to be that of the band tail electrons and the prefactor $\tau_0 = 10^{-8}$ s. A similar expression with a prefactor $\tau_0 = 10^{-12}$ s describes the lifetime for non-radiative recombination τ_{nr}. In case of competing radiative and non-radiative processes the PL efficiency η and the decay time τ are given by

$$\eta = \frac{p_r}{p_r + p_{nr}}, \qquad \tau^{-1} = \tau_r^{-1} + \tau_{nr}^{-1} = p_r + p_{nr}, \tag{2}$$

where p_r and p_{nr} denote the probabilities for radiative and non-radiative recombination. Following these relations η and τ are strongly related.

The most obvious result of alloying is the increase in band-gap energy and broadening of the band tails. Although a contribution of a Stokes shift of one or both carriers cannot be excluded the data will be discussed in terms of the thermalization model only. In this case, the width of the photoluminescence spectrum E_{FWHM} is approximately proportional to the inverse slope of the band tails [22]. On the other hand, the thermalization depth ($\approx E_{04} - E_{PL}$) is related to the slope of the band tails, too, although in a more complex way [23]. Nevertheless — and this is quite a surprise — the quantities plotted in Fig. 4 show the same functional increase with x. A simple model seems to be appropriate, where with increasing x the band tails broaden and therefore the carriers thermalize deeper into the gap and attain a broader energetic distribution. The incorporation of carbon into the amorphous network thus leads to more structural disorder. It is interesting that this effect seems to be not that important at low carbon contents since the band-tail width changes only little at low x ($x < 0.2$). This observation can be related to the fact that in this composition range the hydrogen content increases strongly. It has been suggested that hydrogen atoms do not solely act as bond terminators, but also reduce the distortion of the

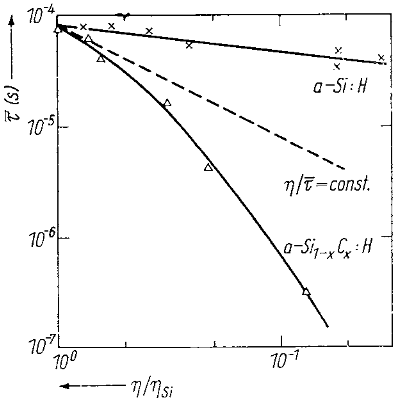

Fig. 11. Average lifetime $\bar{\tau}$ as a function of the normalized quantum efficiency for a-Si:H and a-Si$_{1-x}$C$_x$:H

SiC network and that up to $x \approx 0.45$ the hydrogen content determines the band gap of these films [7]. It is thus reasonable that at least at low x the hydrogen content influences strongly the structural and optical properties of the SiC alloys which therefore should rather be regarded as ternary alloys.

Next we discuss the variation of the quantum efficiency and the decay time with x (Fig. 7 to 9). Both quantities are determined by the non-radiative rate $p_{nr} = 1/\tau_{nr}$ and thus are related to the defect density. The decrease of the quantum efficiency with x usually is attributed to an enhancement of the defect density. The shift of the decay time, however, is much stronger than expected from (2). This is shown in Fig. 11 where $\bar{\tau}$ is plotted as a function of η/η_{Si} and the behavior expected from (2) is shown for comparison by the dashed line ($\eta/\bar{\tau}$ = const). Furthermore, the quantum efficiency increases again at higher x although the films of higher x probably are of minor quality. These observations therefore cannot be explained merely by an increase of the defect density by alloying.

In order to get more insight into the role of defects we have examined the relation of $\bar{\tau}$ and η in a-Si:H films by changing the defect density by particle bombardment and annealing. With the spin density increasing from 3×10^{16} to 6×10^{17} cm^{-3} the quantum efficiency drops by a factor of 30. The surprising result shown in Fig. 11 is that this drastic increase of the defect density has little effect on $\bar{\tau}$ which decreases only by a factor of two. This is consistent with the observation of Collins et al. [24] that the decay of the photoluminescence for times $t > 10$ ns was essentially unaffected by the quality of their sputtered a-Si:H samples. Such behavior suggests that the

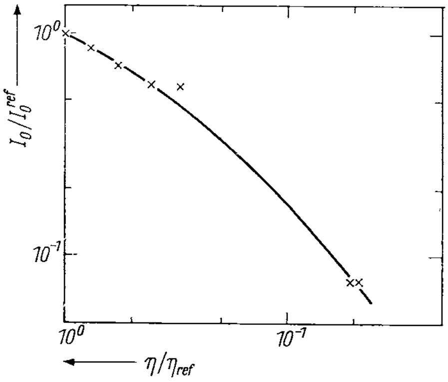

Fig. 12. Initial luminescence intensity I_0 vs. quantum efficiency η of an a-Si:H film. Both quantities are normalized to the values of the film in the annealed state

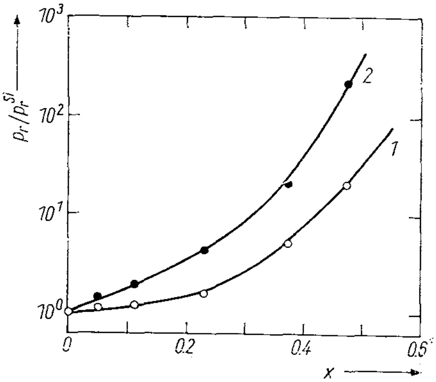

Fig. 13. Probability of radiative recombination (relative to the Si value) as a function of composition x. Calculated from relation (2) for two limiting cases: (1) Non-radiative recombination competes in the time scale of the experiment, (2) non-radiative recombination is fast and non-competitive

dominant non-radiative recombination process is fast and does not compete with radiative recombination on the time scale of this experiment (10^{-8} s $< t < 10^{-3}$ s). Therefore most of the non-radiative recombination must occur at $t < 10^{-8}$ s. One then expects that in the decay curves the initial intensity I_0 ($t = 10^{-8}$ s) decreases strongly with increasing defect density of the films. Fig. 12 shows this behavior in a plot of the intensity I_0 versus the quantum efficiency. It should be emphasized that this interpretation implies that the lifetime distribution of a-Si:H in Fig. 8b reflects the radiative lifetimes only. Hence in a-Si:H the average radiative lifetime here amounts to $\bar{\tau}_r = 1/p_r = 8 \times 10^{-5}$ s. At present one can only speculate about the nature of the fast non-radiative process. A likely mechanism is the direct capture of free or thermalizing carriers at non-radiative centers which are considered to be Si dangling bonds.

In the SiC alloys the situation is obviously more complex: η decreases by about a factor of 10 at $x = 0.47$ but the average lifetime is strongly diminished from 8×10^{-5} s at $x = 0$ to 3×10^{-7} s at $x = 0.47$. This shift of the lifetime spectra is much stronger than predicted by (2). If only defects enhance the non-radiative channel, one would expect $\eta/\tau = p_r =$ const. This behavior is given in Fig. 11 by the dashed line. The obvious discrepancy suggests that in the a-Si$_{1-x}$C$_x$:H alloys in addition $p_r = 1/\tau_r$ is strongly enhanced with increasing x. Fig. 13 shows this increase calculated from (2) on the basis of the assumption that non-radiative recombination competes with radiative recombination on the time scale of the experiment (curve 1). There is, however, no reason why defects should act differently in a-Si:H and a-Si$_{1-x}$C$_x$:H. We therefore rather believe that with increasing x the efficiency decreases because of an enhancement of the fast ($t < 10^{-8}$ s) non-radiative recombination rate and that the shift of the lifetime spectra to shorter times results almost entirely from a strong increase of $p_r = 1/\tau_r$ (curve 2, Fig. 13). This interpretation is in accordance with ps-spectroscopy studies of Masumoto et al. [25] and Nakazawa et al. [26] which point to a radiative lifetime in the order of 10^{-8} s^{-1} in carbon-rich alloys ($x \approx 0.85$). Similar conclusions have been made in a discussion of the temperature dependence of the cw luminescence of a-Si$_{1-x}$C$_x$:H films [19] and of a-SiN$_x$:H films [10]. In the latter case, too, this interpretation is consistent with the observed shift of the lifetime spectra to shorter times [27]. It is interesting to mention that the strong increase of p_r offers a reasonable explanation for the increase of the efficiency at higher x. With increasing carbon content the enhancement of the radiative rate p_r may overcompensate the enhancement of the non-radiative rate p_{nr} which is due to defect production.

Thus we arrive at the conclusion that the radiative lifetime τ_r is drastically reduced by alloying with carbon. According to (1) this means that the intrapair separation of the recombining electrons and holes is smaller in the alloys. Two possible mechanisms can account for this:

1. Since the tail states are broader the faster thermalization may reduce the influence of carrier diffusion.
2. Stronger Coulomb interaction between the recombining carriers enforces stronger localization.

Both of these assumptions are supported by the time-resolved spectra. All of the data indicate flatter band tails with increasing x which leads to faster thermalization due to the larger number of available states. In Fig. 10 enhanced thermalization is visible in the early time regime 10^{-8} s $< t < 3 \times 10^{-7}$ s and the shift of E_{PL} to higher energy in the medium time range points to stronger Coulomb interaction.

Acknowledgement

The authors would like to thank the Bundesministerium für Forschung und Technology for financial support.

References

[1] D. A. Anderson and W. E. Spear, Phil. Mag. B **35**, 1 (1977).
[2] H. Munekata and H. Kukimoto, Appl. Phys. Letters **42**, 432 (1983).
[3] D. Kruangham, T. Endo, W. Guang-Pu, S. Nonomura, H. Okamoto, and Y. Hamakawa, J. non-crystall. Solids 77/78, 1429 (1985).
[4] Y. Tawada, K. Tsuge, M. Kondo, H. Okamoto, and Y. Hamakawa, J. appl. Phys. **53**, 5273 (1982).
[5] A. Morimoto, T. Miura, M. Kumeda, and T. Shimizu, J. appl. Phys. **53**, 7299 (1982).
[6] J. Bullot, M. Gauthier, M. Schmidt, Y. Catherine, and A. Zamouche, Phil. Mag. B **49**, 489 (1984).
[7] W. Beyer, H. Wagner, and H. Mell, in: Materials Issues in Applications of Amorphous Silicon Technology, Ed. D. Adler, A. Madan, and M. H. Thompson, MRS, Pittsburgh (Pa.) 1985 (p. 189).
[8] R. S. Sussman and R. Ogden, Phil. Mag. B **44**, 137 (1981).
[9] R. Carius, K. Jahn, W. Siebert, and W. Fuhs, J. Lum. **31/32**, 354 (1984).
[10] I. G. Austin, W. A. Jackson, T. M. Searle, P. K. Bhat, and R. A. Gibson, Phil. Mag. B **52**, 271 (1985).
[11] R. A. Street and J. C. Knights, Phil. Mag. B **42**, 551 (1980).
[12] W. Siebert, K. Jahn, and W. Fuhs, J. non-crystall. Solids 77/78, 869 (1985).
[13] R. A. Street, Adv. Phys. **30**, 596 (1981).
[14] W. Rehm and R. Fischer, phys. stat. sol. (b) **94**, 595 (1979).
[15] J. Shah, A. Pinczuk, F. B. Alexander, and B. G. Bagley, Solid State Commun. **42**, 717 (1982).
[16] W. A. Jackson, T. M. Searle, I. G. Austin, and R. A. Gibson, J. non-crystall. Solids 77/78, 909 (1985).
[17] P. K. Bhat, T. M. Searle, I. G. Austin, R. A. Gibson, and J. Allison, Solid State Commun. **45**, 481 (1983).
[18] B. Jackson and R. J. Nemanich, J. non-crystall. Solids **59/60**, 353 (1983).
[19] R. S. Sussman and E. H. Lauder, J. Physique **42**, C4-1029 (1981).
[20] C. Tsang and R. A. Street, Phys. Rev. B **19**, 3027 (1979).
[21] R. A. Street, Solid State Commun. **34**, 157 (1980).
[22] F. Boulitrop and D. J. Dunstan, Phys. Rev. B **28**, 5923 (1983).
[23] D. J. Dunstan and F. Boulitrop, Phys. Rev. B **30**, 5945 (1984).
[24] R. W. Collins, P. Victorovitch, R. K. Weisfield, and W. Paul, Phys. Rev. B **26**, 643 (1982).
[25] Y. Masumoto, S. Shionoya, H. Munekata, and H. Kukimoto, J. Phys. Soc. Japan **52**, 3985 (1983).
[26] E. Nakazawa, H. Munekata, and H. Kukimoto, Solid State Commun. **45**, 925 (1983).
[27] W. Siebert, Dissertation, Universität Marburg, 1985.

(Received September 26, 1986)